Gold supported on oxide surfaces: environmental effects as studied by STM

David E. Starr, Shamil K. Shaikhutdinov*, and Hans-Joachim Freund

Department of Chemical Physics, Fritz-Haber-Institut der Max-Planck-Gesellschaft, Faradayweg 4–6, 14195 Berlin, Germany

This paper begins by providing a short review of STM studies of gold particles supported on oxide surfaces. Following this, the morphology of Au particles deposited on thin FeO(111) films at elevated pressures of CO, O_2, CO + O_2, and H_2 has been examined using *in situ* STM at room temperature. The Au particles are found to be quite stable in oxygen and hydrogen environments at pressures up to 2 mbar. However, in CO and CO + O_2 atmospheres, the destabilization of Au particles located at the step edges occurs leading to the formation of mobile Au species, which migrate across the oxide surface. General problems encountered with high-pressure STM studies are discussed, and data clearly showing the effects of ambient gas impurities is provided. These effects may lead to erroneous conclusions, particularly about morphological changes of and CO dissociation on the gold surfaces at elevated pressures.

KEY WORDS: gold; morphology; CO oxidation; hydrogenation; scanning tunneling microscopy.

1. Introduction

Bulk gold has long been regarded as an "inert" material in catalysis. However, gold particles below 5 nm in size have recently received much attention due to their unique catalytic properties [1–4]. As a result, numerous "surface science" studies are currently being performed in order to understand why gold behaves as a catalyst when its dimensions are reduced to the nanometer scale (see review [5]).

Within the surface science approach to catalysis research, well-defined model systems are formed where the catalytic metal of interest is deposited onto an electrically conducting oxide single crystal or a thin metal-oxide film grown on a metal single crystal substrate. This approach allows the exploitation of all the tools of surface science for precise system characterization using electron spectroscopies and scanning tunneling microscopy (STM) while providing systems that more closely represent the real catalysts than metal single crystals. These model systems therefore allow one to bridge the material gap between real catalysts and metal single crystals [6–10].

While there have been many studies of the Au model systems conducted in ultra-high vacuum (UHV), relatively unexplored are potential modifications of these systems in a reactive environment. In this respect, many fundamental questions still remain including the possibility of pressure induced morphological changes in the system. For example, when a metal particle interacts with the reactive gas, a weakening of the metal–metal bonds within the particle may occur that leads to a disruption of

the structure of the metal particle. Also, the strength of interaction between the metal particle and the support may play a significant role in determining the stability of these systems at higher pressures. In addition, the support itself may react with the ambient gas and therefore affect the metal–support interaction. Conducting STM studies at elevated pressures provides the opportunity to directly address these issues.

It is well established that the interaction of gold with gases at elevated pressures is much stronger as compared to those used in UHV studies. Peters *et al.* found by surface X-ray diffraction evidence for lattice expansion of the Au(111) surface exposed to CO at 300 K at pressures between 0.1 and 530 mbar [11], although the "herringbone" surface reconstruction of Au(111) was preserved. More extensive reconstruction of the Au(111) surface was observed when exposed to 110 mbar CO at 600 K. Since the surface disorder remained after evacuation, the authors concluded that irreversible dissociative adsorption must have occurred.

Bertolini and co-workers observed similar behavior for Au(110) at CO pressures above 0.1 Torr [12]. STM results showed significant surface roughening and a lifting of terrace anisotropy. Surprisingly, increasing the CO exposure time suppressed CO adsorption as monitored by infrared spectroscopy. The authors proposed that CO dissociation occurs on the gold surface at high pressures accompanied by carbon deposition.

The same group has recently studied the Au(111) surface in the CO pressure range of 10^{-3} to 10^3 Torr [13]. Again, they observed surface roughening above 100 Torr. It is important to note that the morphological changes observed for both Au(111) and Au(110) surfaces were irreversible upon CO evacuation at room temperature.

* To whom correspondence should be addressed.
E-mail: shaikhutdinov@fhi-berlin.mpg.de

For supported Au model systems, gold deposited on TiO$_2$ rutile(110) is the most widely studied system (see review [14]). At very low coverage, gold grows two-dimensionally at room temperature, which then subsequently changes to three-dimensional growth with increasing coverage [15–18]. At higher deposition temperatures, the growth mode is more 3D from the beginning, implying that the observed 2D growth at low temperatures is a kinetically limited mode [15,18].

It is fairly well established, that for many metal/oxide systems, including supported gold as well, the nucleation of metal particles occurs at defect sites such as step edges, line and point defects [16,17,19]. Recently, Besenbacher and co-workers, studying the relationship between gold particle nucleation and oxygen vacancies on a TiO$_2$(110), using high resolution STM [20], showed that the number of vacancies is drastically reduced upon the deposition of gold. Corroborated by density functional theory (DFT) calculations, these STM results showed that the gold atoms prefer to bind to oxygen vacancies present on the titania surface.

Recently, Goodman and co-workers have studied Au clusters stabilized by surface defects of thin SiO$_2$ and TiO$_x$/SiO$_2$ films grown on Mo(112) [21,22]. Annealing at 700–850 K drives Au clusters from the line defects present on the silica film to form larger particles, which are stabilized primarily on step edges. When small TiO$_x$ islands have been formed on the SiO$_2$ films, the Au clusters nucleate on these islands indicating much stronger interaction of gold with titania than silica.

Egdell and co-workers observed Ostwald ripening (the growth of large particles at the expense of small particles) in their examination of the high temperature stability of gold particles on TiO$_2$(110) with *in situ* STM [23]. This system was monitored by STM and, similar to Pd/TiO$_2$(110) which they previously studied, a shift in the particle size distribution towards larger particles was found. Although many different dynamic processes were observed in the cluster sintering process, clusters of ~5 nm in dimension were stable and the authors felt that the sintering process was dominated by Au atom diffusion.

Kitchin *et al.* also revealed significant sintering upon annealing of gold particles on TiO$_2$(110) to 773 K [24]. The annealed particles appeared to be strongly associated with defects on the TiO$_2$ surface.

A form of Ostwald ripening was observed by Goodman's group when exposing gold particles on TiO$_2$(110) to 10 Torr of oxygen at room temperature [25]. This process appeared to be even stronger in a reactive environment of O$_2$ and CO (10 Torr, 2:1 CO/O$_2$). These results indicate that the ripening processes are intimately connected with the reactivity of the particles; however, the mechanism of the ripening process remains unclear.

Kolmakov and Goodman further studied the sintering behavior of gold on TiO$_2$(110) under reaction conditions with *in situ* STM [26,27]. Morphological changes

of the TiO$_2$(110)−(1x2) surface were observed with prolonged exposures at 10^{-4} Torr of O$_2$ at 300 K which was attributed to the segregation of Ti$^+$ interstitials forming (1×1) islands. An initial uniformly sized group of Au particles was observed to undergo severe Ostwald ripening at 720 Pa and 450 K. The authors suggested that the presence of oxygen served to weaken Au–Au bonds, thereby promoting sintering. Images taken under reaction conditions showed that the behavior of particles that were initially of the same size could be quite different, as some particles decreased in size or even disappeared, while others seemed to remain stable. This work also highlighted the importance of considering tip-induced effects during high-pressure STM studies, including cluster movement by or adhesion to the tip, and also possible gas-induced changes in the tunneling process.

Unlike on TiO$_2$(110), growth of gold on thin alumina films, formed on a NiAl(110) single crystal, is 3-D even at very low coverages [19,28]. The absence of preferential nucleation for deposition at 300 K indicates that the gold atoms have a fairly low mobility on the alumina surface. This is surprising since gold, being a noble metal, was expected to behave similar to Pd and Ag, which showed high mobility on the alumina surface at 300 K [29]. The Au particles were quite stable towards heating up to 600 K, since the particles only slightly sintered.

Iron oxide thin films have only recently begun to attract attention as a suitable oxide substrate for model metal/oxide systems [19,30,31]. The FeO(111), Fe$_3$O$_4$(111) and Fe$_2$O$_3$ (0001) surfaces can be obtained by cycles of iron deposition and subsequent oxidation using a Pt(111) single crystal as a substrate [32].

Similar to other oxide supports, gold deposition on the FeO(111) film first resulted in step decoration [19]. Subsequently, small Au clusters nucleate and grow on the terraces as well. The nucleation density of gold on the FeO film was approximately half that of gold on the Al$_2$O$_3$/NiAl(110) films at the same Au deposition rate. This implies that, even though both oxides are very thin and terminated by oxygen [33,34], gold diffusivity on these supports is quite different. The higher mobility observed for gold on FeO probably results from a lower defect density on the FeO film as compared to alumina. STM studies also showed that gold forms monolayer islands on the FeO(111) surface at low coverage. With increasing amounts of gold, three-dimensional particles up to 7 nm in diameter could be grown [30].

Due to the presence of vacancy defects, gold diffusion on Fe$_3$O$_4$(111) films was found to be rather limited relative to the FeO film. A relatively broad particle size distribution was observed for Au/Fe$_3$O$_4$ at room temperature. However, heating to 500 K caused sintering, better faceting and a narrowing the size distribution with a shift to larger average size, ca. 4 nm [19]. The histogram analysis of STM images for the annealed samples

revealed that particles grow by increasing the number of layers in the cluster. The annealed particles were well ordered exhibiting mostly hexagonal and trigonal shapes. It was concluded that the top facets of the particles expose the (111) surface owing to the small ($\sim$3%) lattice mismatch between the Au(111) and Fe_3O_4(111) surfaces. The STM results for the α-Fe_2O_3(0001) films are very similar to those found on the Fe_3O_4 films: Au particles are homogenously distributed on the oxide surface and exhibit a hemi-spherical shape.

CO adsorption studies on gold deposited onto alumina and iron oxide films performed in our group using TPD and IRAS clearly showed a particle size effect in that small particles adsorb CO more strongly [19,30]. At the lowest Au coverage, CO may desorb at and above room temperatures, which is in the temperature range of the working Au catalysts for low temperature CO oxidation. These strongly bound states have never been observed for Au single crystals and are most likely associated with highly uncoordinated gold atoms present on the surface of the small particles.

Based on their study of various planar Au/FeO_x model catalysts [35], Guczi and co-workers have proposed a CO oxidation mechanism whereby contact between gold and the active oxide phase is essential. They have speculated that the interface between amorphous iron oxide and gold is electron rich, resulting in a favorable site for CO adsorption and oxidation. However, in our own work, we have failed to see unique adsorption sites for CO that must be ascribed to the gold/oxide interface [19,30].

In the present work, we report on *in situ* STM studies of supported gold particles at elevated pressures. In particular, we focus on the Au/FeO(111) system. We found this system to be interesting for several reasons. First, the thin FeO film does not exhibit extended line defects and is shown to be free of point defects such as vacancies, which seems to be very important for both structure and reactivity of Au particles supported on TiO_2 and MgO [20,36]. Therefore, the changes observed, if any, should primarily be associated with the interactions between the gases and the Au particles alone, due to their weak interaction with the support. Secondly, the FeO film typically shows very wide and flat terraces, which aids monitoring structural changes by STM, particularly if the morphology is affected by STM tip and/or highly reactive impurities in the gas feedstock.

2. Experimental

The experiments were performed in an UHV chamber (a base pressure of $<2 \times 10^{-10}$ mbar) equipped with Auger Electron Spectroscopy/Low Energy Electron Diffraction (AES/LEED) (Specs), a Quadrupole Mass Spectrometer (QMS) (Fisons VG) and a STM (Micro H, Omicron) along with standard sample cleaning facilities. The STM is housed in a small chamber separated from the main chamber by a gate valve to allow *in situ* STM measurements in different gas ambient. An additional, Au-plated high-pressure cell is attached to the main chamber allowing treatments similar to those in the STM chamber for *ex situ* measurements. Combining the *ex situ* and *in situ* measurements allows one to ascertain whether observed morphological changes are potentially induced by STM tip modifications at elevated pressure at least in the case of irreversible changes. Commercial Pt/Ir tips (LOT-Oriele GmbH) were used with tunneling currents of ca. 0.7 nA and positive sample biases of ca. 0.2 V. All STM images are presented in the paper in differentiated contrast.

The Pt(111) single crystal was cleaned via cycles of Ar^+ bombardment (1 keV, 2 $\mu A/cm^2$) at 300 K followed by annealing to 1300 K for 3 min. To remove carbon, the sample was annealed in oxygen ($\sim 10^{-6}$ mbar) at 600 K for 5–10 min followed by flashing to 1000 K to desorb oxygen. The clean crystal showed a very sharp (1 × 1) LEED pattern and no detectable impurities by AES. STM images from the clean Pt(111) were used to calibrate STM.

Gold and iron (both 99.99%, Goodfellow) deposition was carried out using a metal evaporator (Focus EFM3). During evaporation, a retarding voltage was applied to the sample in order to prevent any sputter damage caused by accelerated metal ions emanating from the source to the sample. The FeO(111) film on Pt(111) was prepared using a well-established recipe. Briefly, $\sim$1 ML of Fe is deposited onto the Pt(111) crystal at room-temperature followed by annealing at 1000 K for 2 min in $\sim 10^{-6}$ mbar of O_2 through a gold-plated directed doser. The as grown film displayed a characteristic hexagonal superstructure with a $\sim$26 Å periodicity (Moire pattern), clearly visible in STM and LEED, arising from a $\sim$10% mismatch between FeO(111) and Pt(111) lattices [32].

The FeO(111) film is known to be inert to adsorption of background gases. However, to assure cleanliness of the surface before Au deposition, the surface was briefly flashed to 500 K. Gold was then deposited at a rate of $\sim$0.1 Å/min at <110 K. For each Au deposition a new FeO(111) film was grown. Following Au deposition, the sample was transferred to the STM chamber and imaged at room temperature. During the elevated pressure measurements, the gate valve between the main and STM chambers was closed and gas was introduced to the STM chamber via a leak valve. For each "high-pressure" (HP) STM experiments, a new sample was prepared.

Great care was taken to ensure the cleanliness of gases used (CO (4.7, Linde), O_2 (5.0, AGA Gas) and H_2 (6.0, Linde)) through repeated rinsing of the gas handling system and the STM chamber prior to use. In addition, the gas was introduced through a cold trap kept at 77 K for H_2, and $\sim$200 K for O_2. In order to avoid contamination with metal (Fe, Ni) carbonyls, the

CO gas line was equipped with a filter (Wafepure Mini-XL, Mycrolis GmbH). The gas pressure in STM chamber was measured using a cold-cathode and MKS Baratron dual gauge system with overlapping pressure ranges.

3. Results and discussion

Our previous TPD studies of supported Au particles revealed that CO interacts with small Au clusters more strongly than other simple molecules such as H_2, O_2, and ethylene. In particular, as mentioned in the Introduction, data reported in the literature have indicated the possibility of CO dissociation on gold at elevated pressures. To further investigate this phenomenon, we have performed STM measurements of FeO(111) supported Au particles in a CO ambient.

Figure 1 shows 4 snapshots from a STM "movie" ($\sim$5 min per frame) of Au deposited on the FeO(111) film. While recording this movie, the CO pressure was slowly increased such that the images 1, 2, 3 and 4 correspond to CO pressures of 10^{-6}, 10^{-4}, 10^{-3}, and

2 mbar, respectively. Comparing images 1 and 4 clearly indicates that the particles decorating the steps under vacuum conditions, disappear causing the step edges to become "clean" in the mbar-pressure range. Frames 2 and 3 display the system at the transition pressure range when these changes first begin to emerge. One can see that the resolution of image 3 is improved since the step edges become sharper. This can be explained by CO adsorbing on the STM tip, thus making the tip apex "sharper". Due to well-known tip-surface convolution effects, this causes the smallest particles appear smaller with the "CO"-tip, while the effect for the larger particles is rather negligible. In addition, within this pressure range, new very small species appear on the terraces (see the zoomed in portion of figure 1). These features were seen while scanning in both the forward and backward directions and therefore are attributed to species on the surface. With time these species disappear and nearly cannot be seen in image 4. Since the particles on the terraces did not increase in size, the gold species from the step edges have not stuck to any significant extent onto the large particles. It therefore seems plausible that
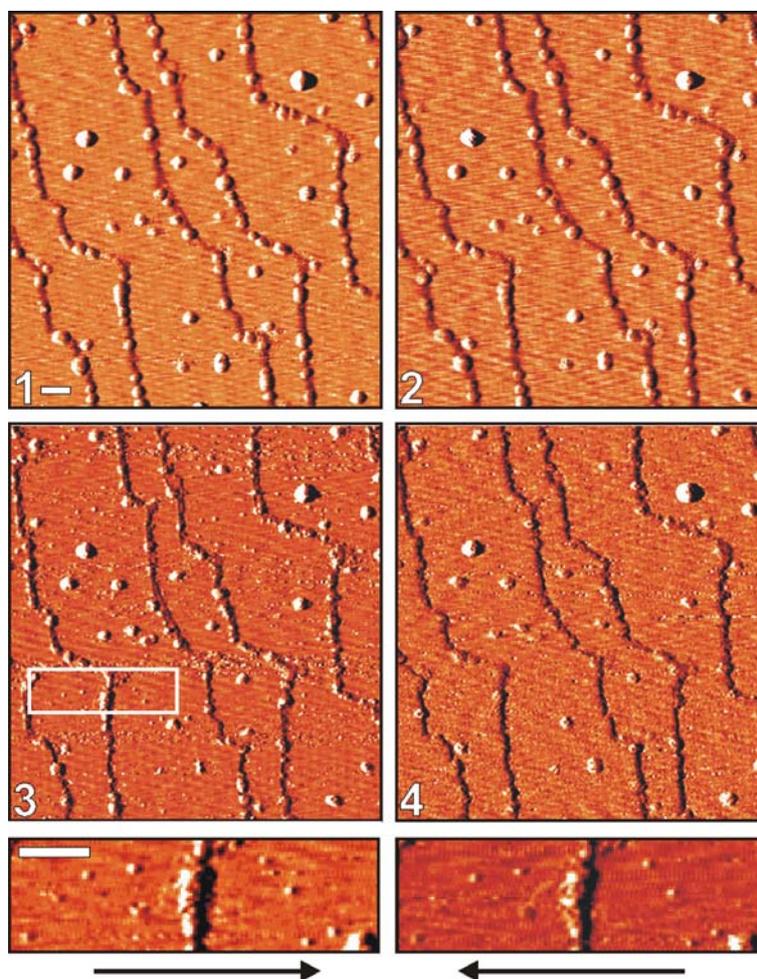
Figure 1. Four snapshots from a series of STM images of Au particles on a FeO(111) thin film taken with increasing CO pressure. The CO pressure is 10^{-6}, 10^{-4}, 10^{-3} and 2 mbar for images 1, 2, 3, and 4, respectively. The bottom two images of the figure displays the close-up of image 3, indicated by the rectangle, imaged in both forward and reverse directions. The scale bar corresponds to 10 nm.

Figure 2. Two snapshots from a series of STM images of Au/FeO(111) taken with increasing O_2 pressure. The O_2 pressure is 10^{-5} and 2 mbar for images (a) and (b), respectively. The scale bar corresponds to 10 nm.
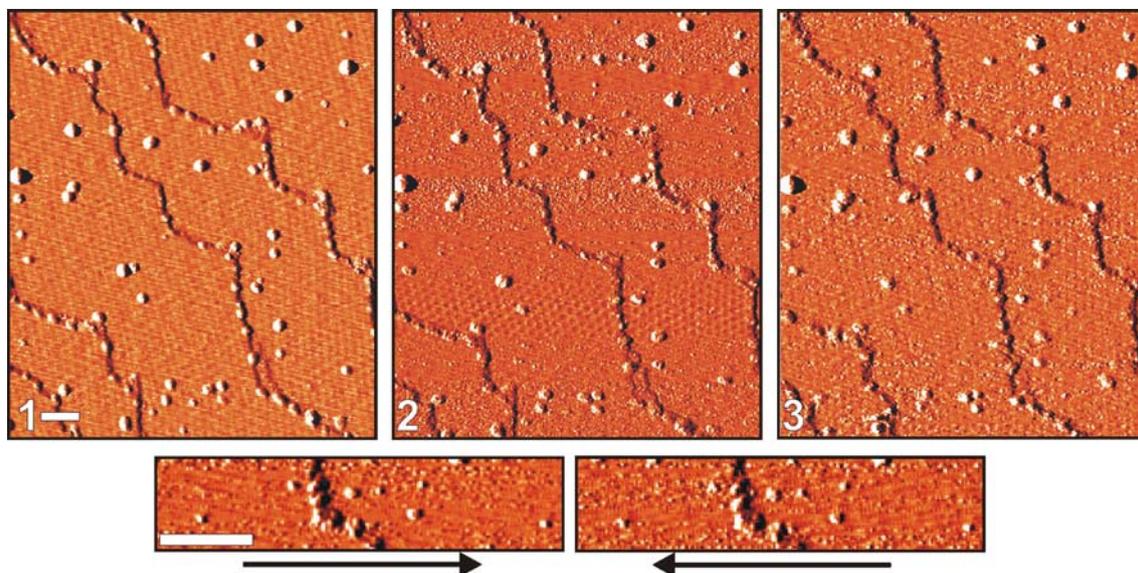
these species are in fact quite mobile on the surface and hence "invisible" in the STM images at elevated pressures. This conclusion is consistent with the observation that after CO was pumped out STM again revealed Au clusters decorating steps.

Based on these observations, we can conclude that, starting in the ca. 10^{-3} mbar pressure range, CO destabilizes the small Au clusters that are present on the step edges and makes them more weakly bound. As a result, these species become mobile or possibly break apart into smaller, more mobile species, which can migrate across the terraces. In principle, this conclusion is consistent with the DFT calculations performed by Piccolo *et al.* [13] that showed that the lower the coordination number of a Au atom is, the lower the pressure needed to achieve a specific CO coverage at room temperature. For example, although it takes ~1 Torr to reach ~0.07 ML coverage on the (874) vicinal Au surface (coordination number 6), for Au adatoms on Au(111) (coordination number 3) a similar coverage can be achieved for pressures as low as 10^{-3} Torr.

The results of similar experiments in O_2 ambient are summarized in figure 2, where two STM images at 10^{-5} and 2 mbar pressures are shown. Essentially, no big changes were observed in the STM-movies during gas exposure. Even though the overall resolution is slightly reduced in the mbar range, the particles were quite stable at all pressures studied. This supports the observation of the relative inertness of the gold particles towards O_2 in our TPD studies under UHV conditions of the same system, where no oxygen was found to chemisorb on the gold particles at temperatures above 80 K.

Figure 3 shows STM images at 10^{-6} (frame 1), 10^{-3} (2), and 2 (3) mbar of $CO + O_2$ (1:1) mixture, respectively. Basically, the changes observed are similar to that of pure

Figure 3. Three snapshots from a series of STM images of Au/FeO(111) taken with increasing pressure in a $CO + O_2$ (1:1) mixed gas ambient. The total pressure is 10^{-6}, 10^{-3}, and 2 mbar for images 1, 2 and 3, respectively. As indicated in the bottom figure, small features attributed to a mobile surface species are observed. The scale bar corresponds to 10 nm.
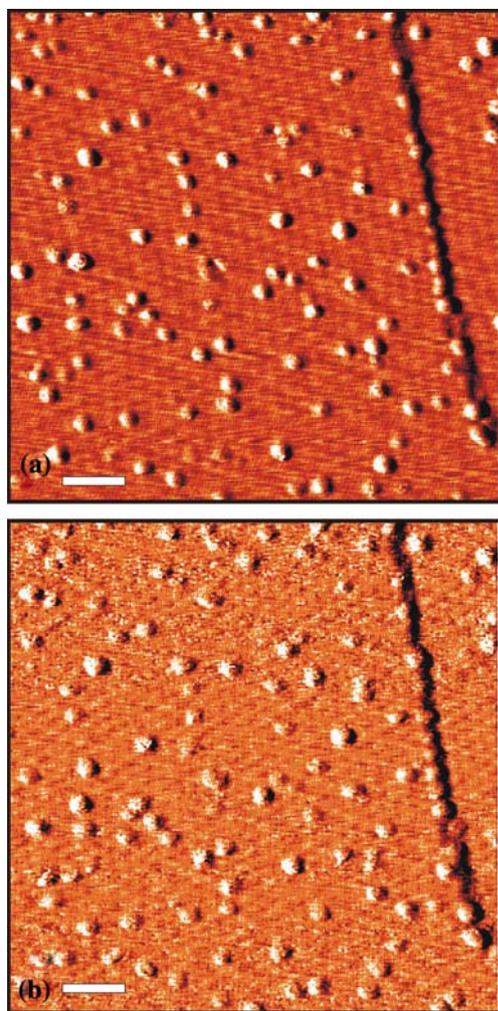
Figure 4. Two snapshots from a series of STM images of Au/FeO(111) taken with increasing H_2 pressure. The H_2 pressure is 10^{-5} and 2 mbar for images (a) and (b), respectively. The scale bar corresponds to 10 nm.

CO (see figure 1). Again, in the 10^{-3} mbar pressure range, small species are observed on terraces as shown in the close-up images of figure 3, which were not seen in vacuum or at lower pressures. However, the removal of the Au species from the steps is less pronounced in the mixed ambient as compared to CO alone. Since oxygen was found not to affect step morphology (see figure 2), this finding may indicate some sort of cooperative effect of CO and O_2 on the gold clusters located at the step edges that increases their stability.

Recently, oxide supported gold has been shown to be a promising catalyst for various hydrogenation reactions (see review [4]). Despite the lack of evidence for hydrogen dissociation on gold surfaces, the activation of hydrogen is thought to be the rate-limiting step. Therefore, studying the behavior of gold particles in a hydrogen atmosphere is of current interest.

Two snapshots of a STM movie are presented in figure 4 at 10^{-5} (a) and 2 (b) mbar of H_2. Similar to what was observed for oxygen, there are no drastic changes in system morphology at elevated pressures. This is consistent with our TPD studies of hydrogen interaction with Au/FeO, in which no hydrogen desorption signal was observed in the spectra following H_2 exposure at 80 K at all gold coverages.

Over the course of these experiments, we have observed that the STM results at elevated pressures are strongly affected by the purity of gases used. This effect is illustrated in figure 5. Images (a–c) show a few snapshots from the STM-movie for the Au particles, which were exposed to CO (99.995% purity) as supplied, i.e. without any additional purification. First, we have observed decoration of steps by some ill-defined features. As a result, the small species, as displayed in figures 1 and 2, are not observed. Second, the particle volume increases on average by a factor of two for particles of 1 nm in height. Image (b) clearly shows how the particles grow "in time" (slow scanning is from bottom to top) along with the simultaneous step decoration. Third, the corrugation amplitude of the Moire pattern of the FeO surface seen between gold particles is strongly enhanced from a typical value of 0.2 Å to about 2.5 (!) Å at the same tunneling parameters. These effects were irreversible, i.e. after CO evacuation the system morphology stays the same. We have checked that these effects are not due to changes of the tip since the same phenomena have been observed in *ex situ* experiments whereby the gas exposure was first performed in the separate HP cell and then studied by STM in vacuum. Finally, the clean, gold-free FeO films also exhibited step decoration when exposed to "contaminated" CO.

The fact that the particle size has significantly increased would seem to indicate particle sintering. However, neither significant changes in particle density nor particle disappearance was observed over the area scanned. This implies that the swelling of the Au particles has been induced by CO. For example, one could suggest that CO decomposes on the gold particles accompanied by carbon deposition. CO dissociation at high pressures has been previously suggested to occur on gold single crystal surfaces [12,13]. Indeed, AES spectra of the Au/FeO system, shown in figure 6, revealed traces of carbon following HP exposure to unpurified CO. However, knowing the results shown above for the purified CO, we conclude that the swelling effect is not induced by CO but instead by impurity contained in the CO feedstock.

Many researchers are aware of volatile metal carbonyls always present in CO vessels. Our AES results are not conclusive about the presence of Ni and/or Fe carbonyls on the surface after CO evacuation. However, experiments performed with a molecular beam/infrared spectroscopy apparatus in our laboratory have clearly shown the accumulation of CO species with stretching frequencies characteristic for carbonyls during long exposures of "inert" oxide films to non-purified CO [37].
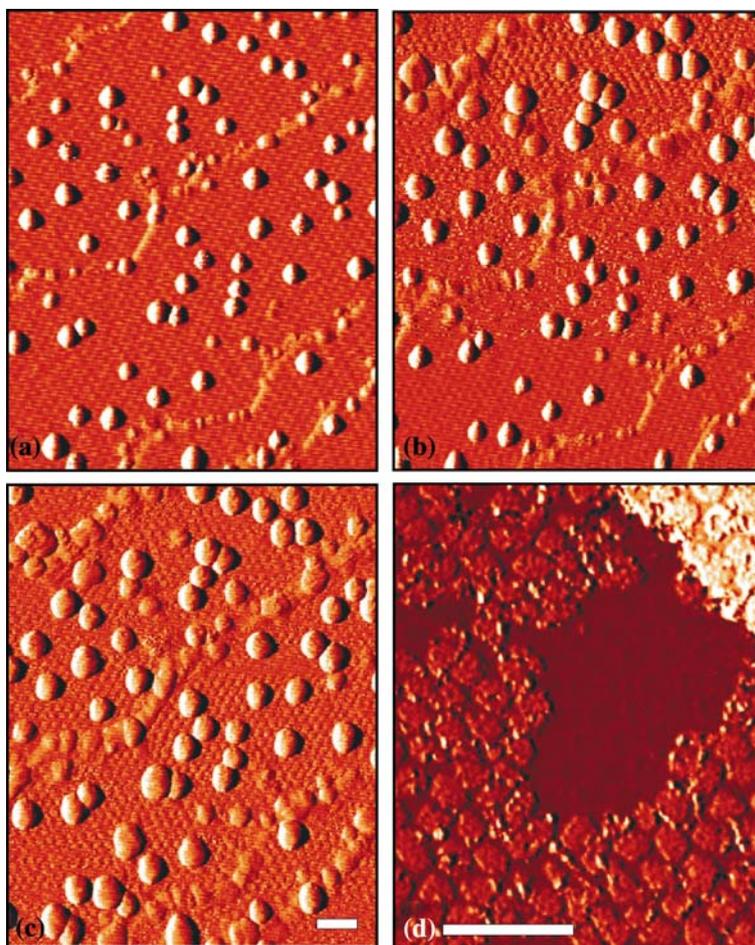
Figure 5. Impurity induced effects on the morphology of Au particles on a FeO(111) thin film during elevated pressure STM in unpurified CO (images a, b and c) and O_2 (image d) ambient. In images (a), (b) and (c), the CO pressure is 10^{-5}, 5×10^{-3}, and 0.1 mbar, respectively. In image (d), the sample has been exposed to 2 mbar of O_2 subsequently pumped out and imaged at UHV conditions. The scale bar corresponds to 10 nm.
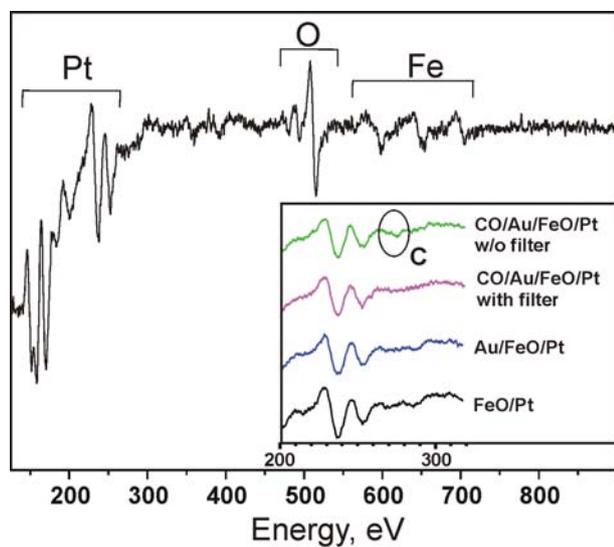
Figure 6. Typical survey AES spectrum of Au/FeO system after HP STM studies. The inset shows the low energy region of AES spectra highlighting the trace of carbon remaining on the surface following exposure to unpurified CO gas at 2 mbar.
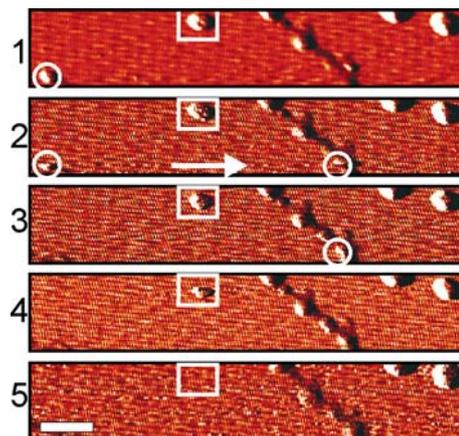
Figure 7. Images cropped from a sequence of STM images taken in a CO ambient highlighting the gradual shrinkage of a small Au particle (square). The circle and arrow indicate tip-induced movement of a small gold particle from the terrace to the step edge. The scale bar corresponds to 10 nm.

Therefore, we believe that the effects observed with unpurified CO at elevated pressures and high exposures on the morphology of the oxide supported gold particles (see figure 5) are due to metal carbonyls rather than CO. Regardless of the nature of the contamination, "impurity" issues may be very important in the behavior of gold catalysts under real catalytic conditions, where such purified gases are not used.

Interestingly, the FeO films, which were exposed to non-purified O_2 (99.999%) showed periodic surface decoration of the Moire superstructure. These species remain on the surface even after the O_2 is pumped out as seen in figure 5d. Together with the observation of a enhanced corrugation amplitude of the FeO surface exposed to unpurified CO, this implies preferential adsorption of the strongly adsorbing impurities at specific sites of the Moire structure. In connection with this, recent low temperature (4 K) STM studies performed in our laboratory have shown that gold single atoms form periodic structures on the FeO surface since gold occupies the sites which possess the highest dipole moment normal to the surface within the Moire unit cell [38]. This results in the greatest reduction of the polar instability of the FeO(111) thin film upon metal adsorption. Therefore, it seems plausible that the adsorption of impurities follows the same mechanism and gives rise to the periodic structure observed in STM images as Moire pattern decoration.

Finally, figure 7 shows a sequence of STM images, which were cropped in order to highlight the gradual shrinkage of a Au particle in CO ambient as marked by the square. The same behavior was observed while scanning in the reverse direction, thus confirming that this effect is not induced by the tip. A tip effect is marked in the same image by the circle showing the movement of a small cluster by the tip to the step edge as indicated by the arrow. However, such events were rarely observed, thus indicating that relatively large ($\sim$3 nm) gold particles are quite stable at room temperature on the FeO(111) film in all ambients studied.

4. Summary

In this paper, we have briefly reviewed STM studies of gold particles supported on oxide surfaces. *In situ* STM studies are becoming increasingly more important in understanding the unique catalytic properties of supported Au nanoparticles.

Specifically, we have studied Au particles deposited on thin FeO(111) films at elevated pressures of CO, O_2, CO + O_2, and H_2 at room temperature. In general, the Au particles appeared to be quite stable in oxygen and hydrogen environments at pressures up to 2 mbar. However, in CO and CO + O_2 atmospheres we observed changes in the morphology of the particles located at step edges. These results have been rationalized through assuming the formation of mobile gold species in CO ambient.

We have also highlighted general problems of STM studies at high pressures where trace impurities of the gas feedstock might play a big role in system behavior and data interpretation. In particular, we have provided direct evidence showing impurity driven morphological changes, which may be incorrectly interpreted as the result of CO dissociation on the surface of the gold particles at elevated pressures.

References

[1] M. Haruta, Catal. Today 36 (1997) 153.
[2] M. Haruta, Chem. Record. 3 (2003) 75.
[3] G.C. Bond and D.T. Thompson, Catal. Rev.: Sci. Eng. 41 (1999) 319.
[4] G.C. Bond and D.T. Thompson, Gold Bull. 33 (2000) 41.
[5] R. Meyer, C. Lemire, S. Shaikhutdinov and H.-J. Freund, Gold Bull. 37 (2004) 72.
[6] D.W. Goodman, J. Phys.Chem. 100 (1996) 13090.
[7] C.T. Campbell, Surf. Sci. Rep. 27 (1997) 1.
[8] C.R. Henry, Surf. Sci. Rep. 31 (1998) 231.
[9] P. Gunter, J.W. Niemantsverdriet, F. Ribeiro and G. Somorjai, Catal. Rev.: Sci. Eng. 38 (1997) 77.
[10] H.-J. Freund, M. Bäumer and H. Kuhlenbeck, Adv. Catal. 45 (2000) 333.
[11] K.F. Peters, P. Steadman, H. Isern, J. Alvarez and S. Ferrer, Surf. Sci. 467 (2000) 1007.
[12] Y. Jugnet, F.J. Cadete Santos Aires, C. Deranlot, L. Piccolo and J.C. Bertolini, Surf. Sci. 521 (2002) L639.
[13] L. Piccolo, D. Loffreda, F.J. Cadete Santos Aires, C. Deranlot, Y. Jugnet, P. Sautet and J.C. Bertolini, Surf. Sci. 995 (2004) 566.
[14] F. Cosandey and T. Madey, Surf. Rev. Lett. 8 (2001) 73.
[15] L. Zhang, R. Persaud and T.E. Madey, Phys. Rev. B56 (1997) 10549.
[16] A.K. Santra, A. Kolmakov, F. Yang and D.W. Goodman, Japan. J. Appl. Phys. 42 (2003) 4795.
[17] N. Spiridis, J. Haber and J. Korecki, Vacuum 63 (2001) 99.
[18] S.C. Parker, A.W. Grant, V.A. Bondzie and C.T. Campbell, Surf. Sci. 441 (1999) 10.
[19] S. Shaikhutdinov, R. Meyer, M. Naschitzki, M. Bäumer and H.-J. Freund, Catal. Lett. 86 (2003) 211.
[20] E. Wahlström, N. Lopez, R. Schaub, P. Thostrup, A. Rønnau, C. Africh, E. Laegsgaard, J.K. Nørskov and F. Besenbacher, Phys. Rev. Lett. 90 (2003) 026101.
[21] B.K. Min, W.T. Wallace, A.K. Santra and D.W. Goodman, J. Phys. Chem. B 108 (2004) 16339.
[22] W.T. Wallace, B.K. Min and D.W. Goodman, J. Mol. Catal. A 228 (2005) 3.
[23] C.E.J. Mitchell, A. Howard, M. Carney and R.G. Egdell, Surf. Sci. 490 (2001) 196.
[24] J.R. Kitchin, M.A. Barteau and J.G. Chen, Surf. Sci. 526 (2003) 323.

[25] X. Lai and D.W. Goodman, J. Mol. Catal. A: Chem. 162 (2000) 33.

[26] A. Kolmakov and D.W. Goodman, Catal. Lett. 70 (2000) 93.

[27] A. Kolmakov and D.W. Goodman, Surf. Sci. 490 (2001) L597.

[28] C. Winkler, A. Carew, R. Raval, J. Ledieu and R. McGrath, Surf. Rev. Lett. 8 (2001) 693.

[29] M. Bäumer and H.-J. Freund, Progr. Surf. Sci. 61 (1999) 127.

[30] C. Lemire, R. Meyer, S. Shaikhutdinov and H.-J. Freund, Surf. Sci. 552 (2004) 27.

[31] R. Meyer, S. Shaikhutdinov and H.-J. Freund, Z. Phys. Chem. 218 (2004) 905.

[32] W. Weiss and W. Ranke, Progr. Surf. Sci. 70 (2002) 1.

[33] Y.J. Kim, C. Westphal, R.X. Ynzunza, Z. Wang, H.C. Galloway, M. Salmeron, M.A. Hove and C.S. Fadley, Surf. Sci. 416 (1998) 68.

[34] G. Kresse, M. Schmid, E. Napetschnig, M. Shishkin, L. Köhler and P. Varga, Science 308 (2005) 1440.

[35] L. Guczi, D. Horváth, Z. Pászti and G. Petõ, Catal. Today 72 (2002) 101.

[36] A. Sanchez, S. Abbet, U. Heiz, W.D. Schneider, H. Häkkinen, R.N. Barnett and U. Landman, J. Phys. Chem. A 103 (1999) 9573.

[37] G. Rupprechter, H. Unterhalt, M. Morkel, P. Galletto, L. Hu and H.-J. Freund, Surf. Sci. 502–503 (2002) 109.

[38] N. Nilius, E.D.L. Rienks, H.-P. Rust, H.-J. Freund, submitted.